Materials and Design 50 (2013) 491–496

Contents lists available at SciVerse ScienceDirect

Materials and Design

journal homepage: www.elsevier.com/locate/matdes

Eddy current nondestructive evaluation of dual phase steel

Sadegh Ghanei *, Mehrdad Kashefi, Mohammad Mazinani

Department of Materials Engineering, Faculty of Engineering, Ferdowsi University of Mashhad, Mashhad, Iran

ARTICLE INFO

Article history:
Received 5 January 2013
Accepted 6 March 2013
Available online 20 March 2013

Keywords:
Composite type microstructure
Dual phase steel
Eddy current testing
Martensite
Material characterization

ABSTRACT

This study proposes eddy current testing (ECT) as a tool for nondestructive material characterization. In the present study, different dual phase steels (DPSs) with different martensite phase percentages were manufactured using various intercritical annealing temperatures (from 745 to 890 °C). The aim of the present study is to correlate ECT outputs with the different percentages of martensite and find a relation for determination of martensite percentage of any unknown DPS sample. Increasing the intercritical annealing temperature leads to an increase in the percentage of martensite in DPS, which it caused to a decrease in magnetic permeability of DPS and subsequent decreasing of ECT outputs. Mechanical properties of DPS specimens can also be predicted by the means of ECT. The study revealed that a good correlation exists between ECT outputs and microstructural and mechanical changes in the DPS specimens ($R^2 > 0.85$) and it shows potential of using ECT for prediction of material properties in the DPS.

1. Introduction

Dual phase steels (DPSs) are being increasingly used by the automotive industries as a suitable alternative for plain carbon steel components. The goal of using this kind of steel is related to the need to the materials with a combination of high strength and good ductility. Weight reduction, fuel saving and an improved safety of the vehicles are some of the beneficial application of DPSs in automotive industries [1].

DPS have a microstructure consisting of a hard second phase (martensite) dispersed throughout the ductile matrix (ferrite) and their microstructure can be compared with a composite composed of a ferritic matrix reinforced by small islands of martensite [2]. DPS form just like a low strength steel due to the low yield stress but they also have a high tensile strength due to their rapid work hardening rate [3]. It is therefore possible to obtain combination of good ductility and high strength which is impossible in the conventional steels [4].

This composite type microstructure can be achieved in all low-carbon steels by intercritical annealing heat treatment in austenite–ferrite region followed by rapid cooling to room temperature in order to transform the austenite to martensite.

Many of the researchers have been reported the martensite phase percentage as one of the most important factor that can greatly affect the mechanical properties of DPS. According to their findings, higher volume fraction of martensite results in an increase in the hardness, yield and ultimate tensile strengths of DPS while the total elongation of them decreases. For instance, Ahmad et al. [5] concluded that increasing the intercritical annealing temperature, leads to an increase in the percentage of martensite in DPS, which in turn results in an increase in the ultimate tensile strength of DPS. Marder [6] found a linear relationship between the both ultimate tensile strength and uniform elongation of DPS and martensite volume fraction. In addition, a linear relationship between the yield strength and martensite percentage was also reported by Kim and Thomas [7]. Moreover, Bhagavathi et al. [8] and Meng et al. [9] have reported an increase in the hardness of DPS with increasing the martensite volume fraction.

Determination of martensite phase percentage is important in this connection. There are two methods for measuring the percentage of martensite phase. First method is metallographic observation by optical microscope which is destructive, expensive and also time consuming. Another method of evaluation uses eddy current testing (ECT), nondestructively. This method is based on the induction of eddy currents in the test specimen in a vortex-like flux pattern by a coil [10]. The formed eddy currents generate a secondary magnetic field, which reacts with the primary field that the coil is generating. Any changes in the electromagnetic field of coil is measurable [11].

ECT is one of the oldest methods of nondestructive testing (NDT) but it has been introduced in the past few years as an industrial tool for microstructural inspections. ECT has a great potential to be a reliable and cost effective alternative to traditional techniques of quality control. Magnetic response of steel parts is sensitive to their microstructure. By calibrating the ECT outputs, any change in microstructure could be detected. In the authors' pervious articles, eddy current method was used for quality control of the heat treated parts, and it was shown that they can be separated based on their grain size [12]. In addition, the application of ECT for

* Corresponding author. Tel./fax: +98 5118763305.
E-mail address: Sadegh.Ghanei@stu.um.ac.ir (S. Ghanei).

0261-3069/$ - see front matter © 2013 Elsevier Ltd. All rights reserved.
http://dx.doi.org/10.1016/j.matdes.2013.03.040

determination of surface carbon content of the carburized steel parts was studied, and the results showed an acceptable accuracy in comparison to the conventional destructive method [13]. Khan et al. [14] found that ECT can be used for evaluation of pearlite percentages in low to high plain carbon steels. Konoplyuk [15] used this method for estimation of the pearlite percentage in ductile cast irons. Also, Konoplyuk et al. [16] applied eddy current method for evaluation of ductile cast irons and showed that this nondestructive method can successfully predict mechanical properties of cast irons. Yin et al. [17,18] employed multi-frequency electromagnetic sensor for measurement of ferrite percentage in ferritic and austenitic stainless steel hot isostatically pressed parts and different outputs were studied. Moreover, they investigated the degree of anisotropy of the microstructure in their samples [19].

The aim of the present work was to correlate eddy current testing outputs (impedance and harmonics) with the different percentages of martensite and find a relation for determination of martensite percentage of any unknown DPS sample. Furthermore, this method was used for prediction of mechanical properties of DPS (hardness and tensile).

2. Experimental procedure

Cold rolled low carbon steel with a thickness of 1.3 mm was used in this investigation as the starting material with an initial microstructure of ferrite and pearlite. The chemical composition of investigated steel was Fe–0.08C–0.41Mn–0.502Si–0.091P–0.232Ni–0.389Cr–0.324Cu (wt pct). The specimens were prepared with a dimension of 200 mm × 20 mm.

Cold rolled steels normalized at 950 °C for 20 min. In order to produce dual phase microstructures containing different volume fractions of martensite phase, steel plates were held in the various intercritical annealing temperatures of 745, 750, 765, 782, 802, 810, 820, 832, 850 and 890 °C for 15 min and subsequently quenched in brine solution. Fig. 1 shows the designed DPS heat treatment cycles which used in this study.

Metallographic samples were cut and polished from heat treated specimens and etched in a solution obtained by dissolving 10 g sodium metabisulfite in 100 mL distilled water. Martensite phase percentage in each sample measured using the Clemex image analysis software.

Tensile test was carried out according to ASTM: E8M standard using Zwick/Z250 testing machine at strain rate of 0.002 s^{-1}, and stress–strain plots were obtained for each sample.

According to ASTM: E384 standard, Vickers's hardness tests were carried out at 10 kg load for 30 s using Avery-Denison testing machine with square-based pyramidal-shaped diamond indenter with face angles of 136°. Hardness tests were performed on the flat specimen with a polished surface. Average of at least 10 hardness measurements has been reported for each specimen.

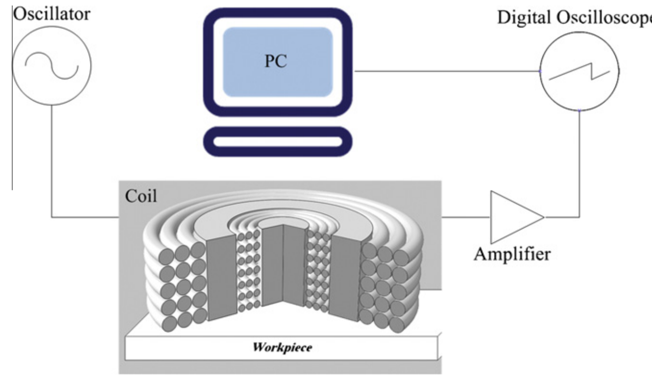

Fig. 2. Principle of the used eddy current circuit.

The eddy current tests were carried out using a tailor-made device [12,13,20] interfaced to a computer for data acquisition (schematic diagram was shown in Fig. 2). The device can apply sinusoidal currents over a wide range of frequencies (0.5 Hz–5 MHz) to the coil. Designs of excitation and pick-up coils were done with respect to the shape of sample. Pick-up coil with 500 turns of 0.2 mm insulated copper wire was wounded on a ferritic cylinder. Height, inner and outer radiuses of this coil was 5.5, 3.5 and 7.5 mm, respectively. Excitation coil (180 turns of 0.3 mm insulated copper wire) was wounded on a ferritic core with the same height and inner and outer radiuses of 11.8 and 15 mm.

The eddy current tests were conducted at room temperature with the lift-off distance (the distance between coil and specimen) of zero. In order to determine the optimum frequencies, preliminary measurements on impedance and harmonic outputs were made with a variety of frequencies from 100 to 1000 Hz and the best excitation frequencies were determined by regression analysis.

3. Results and discussion

3.1. Microstructure analysis and mechanical properties

For all specimens, the microstructure before intercritical annealing consisted of ferrite and pearlite.

When the specimen is heated to the $\alpha + \gamma$ region, austenite forms and due to the following rapid quenching, transformation of austenite to martensite phase takes place and composite type microstructure of martensite and ferrite is obtained. Due to the primary normalization of dual phase steel specimens, there was no banding (anisotropy) and martensite islands have a finely dispersed globular morphology. Fig. 3 shows the microstructure of dual phase specimen with 40% martensite phase (dark area

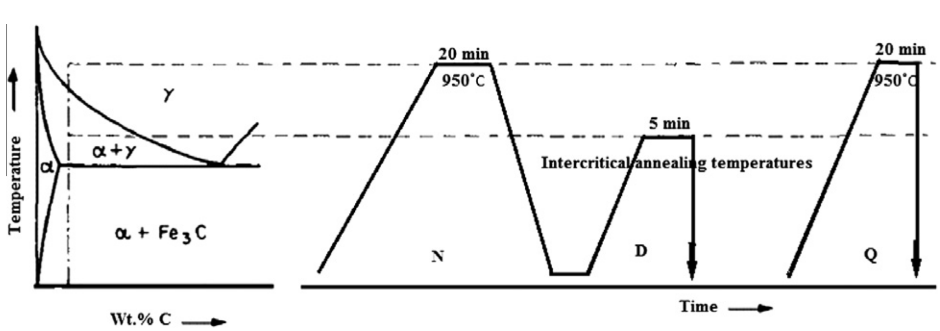

Fig. 1. Schematic of the heat treatment cycles of experiment.

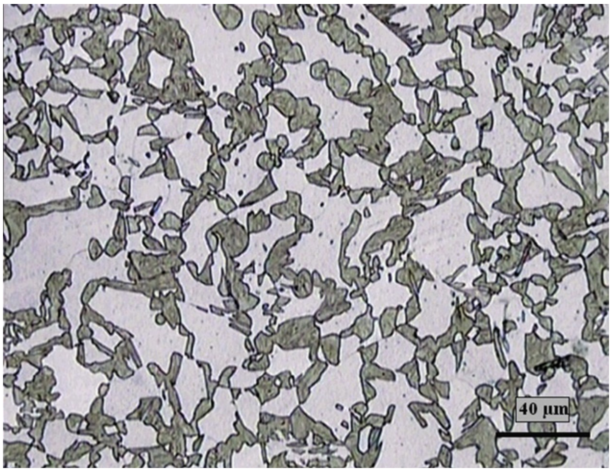

Fig. 3. Optical microscopic image of dual phase microstructure resulted from intercritical annealing at 820 with 40% of martensite phase.

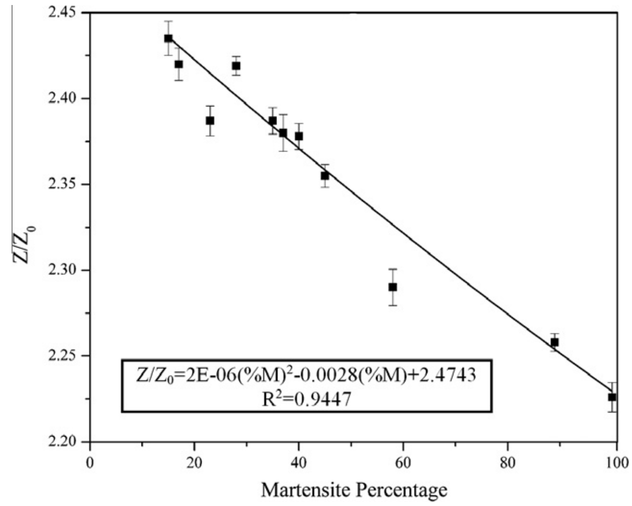

Fig. 4. Plot of the normalized impedance of the coil versus different martensite percentages in the optimum frequency of 250 Hz.

indicates the martensite phases and ferrite phases are illustrated with white color).

Different dual phase samples were produced employing various intercritical annealing temperatures of 745, 750, 765, 782, 802, 810, 820, 832, 850 and 890 °C. The variation of martensite percentage with the intercritical temperature is presented in Table 1. As expected, an increasing in the intercritical annealing temperature results in an increase in the martensite phase percentage. This is due to the larger amount of austenite phase formed at higher temperatures. According to the lever rule [21] in the ferrite–austenite region, by increasing the annealing temperature larger amounts of austenite phase generated, which transforms into martensite on subsequent quenching.

The presence of martensite is the main reason for higher hardness of DPS specimens compared to the normalized ones [8]. Hardness values of DPS are also listed in Table 1. As can be seen, increase in the martensite phase percentage results in an increase in the Vickers's hardness number (VHN) of DPS samples from D-15 to Q-100.

The results of tensile tests (Table 1) indicate that the yield and ultimate tensile strengths of dual phase steel samples increase as the martensite volume fraction in their microstructures increases while their total elongation decreases which are consistent with the results of the previous investigations [5–7]. Due to the presence of hard martensite phase within the ferritic matrix, DPS samples exhibit no yield point phenomenon in their tensile stress–strain curves [8]. Tensile stress–strain curves of the dual phase samples in this investigation (D-15 to D-58) have shown no yield point phenomenon suggesting that the dual phase microstructures have been successfully produced by the intercritical annealing cycles mentioned in Section 2.

3.2. Eddy current study

Flowing of alternative current through a coil causes an alternative magnetic field around it. When the samples are placed in the electromagnetic field of a coil, electrons in the samples circulate in a vortex-like flux pattern, and they form eddy currents. Eddy currents formed in this way, generate a secondary electromagnetic field which reacts with the primary field of the coil. Therefore, it can cause measurable changes in the electromagnetic field that the coil is generating [22].

These changes depend on the magnitude of eddy currents. Induced eddy currents are a function of electromagnetic parameters such as test frequency, electrical conductivity and magnetic permeability of the sample, as well as physical parameters such as the distance between coil and specimen (lift-off), edge effect and skin effect [23,24]. In the present study, test frequency and physical parameters are fixed and electrical conductivity and magnetic permeability are the only effective parameters that can change the response of material to the induced current. The changes in respond of samples are detected by impedance changes.

Frequency determination is the first step for ECT. There are two methods for determining the optimum frequency [20]: 1-using the equation of electromagnetic skin depth, 2-applying regression analysis between material properties and ECT outputs.

In the first method, the equation for calculation of the electromagnetic skin depth (δ), where the magnetic field drops to 37% of its maximum value, is expressed as [16,20,25]:

$$\delta_{(f,\mu,\sigma)} = \frac{1}{\sqrt{\pi f \mu \sigma}} \quad (1)$$

where f is the frequency, σ is the conductivity and μ is the permeability. Applying the first method is not possible due to the different values of σ and μ for DPS samples with different percentages of martensite. Therefore, this method cannot provide a fixed frequency for a fixed depth.

In order to determine the optimum frequencies by the second method, a sinusoidal shaped current with a wide range of

Table 1
Heat treatment temperatures for producing different martensite percentages and the corresponding results of the experiments.

Specimen name	D-15	D-17	D-23	D-28	D-35	D-37	D-40	D-45	D-58	D-89	Q-100
Heat treatment temperature (°C)	745	750	765	782	802	810	820	832	850	890	950
Martensite percentage (%)	15	17	23	28	35	37	40	45	58	89	100
Hardness (Vickers)	201	205	215	229	245	251	257	259	267	339	380
Yield strength (MPa)	410	398	400	405	401	433	440	466	482	–	782
Ultimate tensile strength (MPa)	646	660	676	680	695	690	720	743	756	–	989
Elongation (%)	10.37	9.92	9.86	9.9	9.16	7.95	7.9	7.65	7.47	–	4.78

Table 2
Values of vector modulus of the harmonics 3, 5 and 7 as a function of martensite percentage.

Specimen name		D-15	D-17	D-23	D-28	D-35	D-37	D-40	D-45	D-58	D-89	Q-100
Vector modulus = Π	3	35.25	32.55	32.85	31.92	30.09	29.86	29.55	28.64	27.66	23.66	23.41
	5	35.75	33.07	33.48	33.31	30.29	30.23	31.05	28.25	27.99	24.13	23.23
	7	37.97	34.76	33.60	34.57	32.33	31.30	30.87	30.60	29.28	24.72	24.12

frequency from 100 Hz to 1000 Hz was applied to the coil (this range was used because it results in a good output resolution [14]) for all samples and the preliminary measurements on the impedance (Z) as well as the harmonic were made. The optimum frequency has been determined by applying regression analysis and choosing a frequency with the best correlation coefficient.

According to the regression analysis, frequency of 250 Hz was chosen as the optimum frequency for impedance output. Normalized impedance was determined by dividing the impedance (Z) by the impedance of the empty coil (Z_0) [10,13]. In Fig. 4, the relationship between the normalized impedance and the martensite percentage is shown by a mathematical equation and a correlation coefficient. For the obtained equation, the amount of correlation coefficient is very high ($R^2 = 0.9447$) and this higher accuracy can help to separate the good heat treated samples and the bad ones based on the martensite percentage, carefully. For prediction of martensite percentage with a good accuracy, it is only necessary to nondestructive evaluate of unknown sample by eddy current device and put the obtained impedance into the equation. As can be seen in the figure, values of the normalized impedance decrease with an increase in the martensite phase percentages. Magnetic responses are affected by the microstructure [13,25]. Magnetic permeability of martensite phase is less than ferrite phase [20,26] and so an increase in the martensite percentage results in a decrease in the magnetic permeability of material. This leads to a reduction in the impedance according to the following equations:

$$L = \mu N^2 A / l \tag{2}$$

$$X_L = 2\pi f L \tag{3}$$

$$Z = \sqrt{X_L^2 + R^2} \tag{4}$$

where L, μ, N, A, l, X_L, R and Z are, respectively, the self-induction coefficient, the magnetic permeability, the coil turns, the cross section area, the coil length, the induction resistance, the resistance and the impedance, [18,20,25].

According to Eqs. (2)–(4), increasing the magnetic permeability, leads to an increase in the self-induction coefficient, which, in turn, results in an increase in the induction resistance and a corresponding increase in the impedance output. It should be noted that the effect of μ is stronger than that of R in Eq. (4) [10,13].

Another output of eddy current device is harmonic output which is used here for determination of martensite percentage. Kahrobaee et al. [20] stated the basis of the harmonic analysis of eddy current signals. Based on their report, secondary electromagnetic field (due to the magnetic behavior of the material results from the induced eddy currents inside of the material) affects the primary electromagnetic field of excitation coil in opposite direction. Different magnetic properties influence the amplitude of the harmonic output signals.

Thus, this output implies a method which determines electromagnetic measurable values of DPS which are closely connected to the microstructural changes of DPS. In order to obtain harmonics output, the eddy current device subjects the voltage signal from the probe to the fast Fourier transformation (FFT). Generalized form of the continuous Fourier transform is defined by the complex number:

$$F(x) = \int_{-\infty}^{\infty} f(t) \cdot \exp^{-i2\pi xt} dt, \quad \text{for every real number } x \tag{5}$$

where the independent variable of t represents time and the transform variable of x represents frequency.

By applying Fourier transform on the voltage output signals, main signals can be decomposed into its constituent frequencies and any harmonic components of the input signal are achieved. In the present work, only harmonics of 3, 5 and 7 are used to determine the martensite phase percentages of DPS. After calculating the real (Re) and imaginary (Im) parts, modulus (Π) of each harmonic can be achieved according to the following equation:

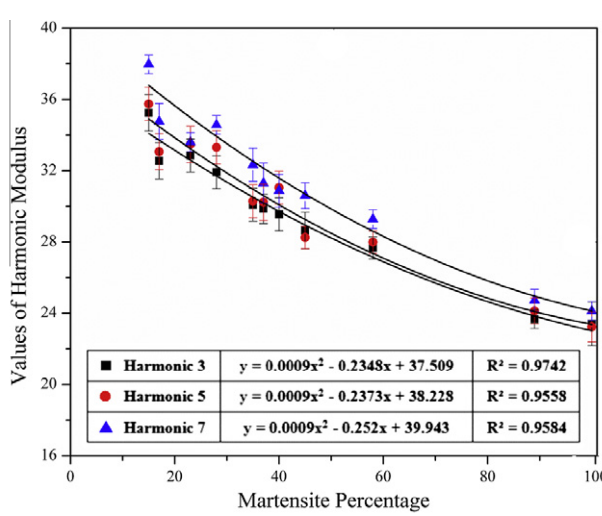

Fig. 5. Variation curves of vector modulus of the harmonics 3, 5 and 7 versus martensite percentage.

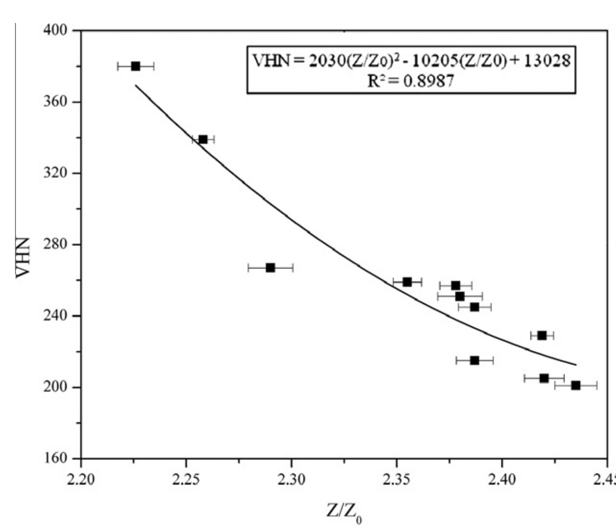

Fig. 6. Vickers's hardness changes with normalized impedance.

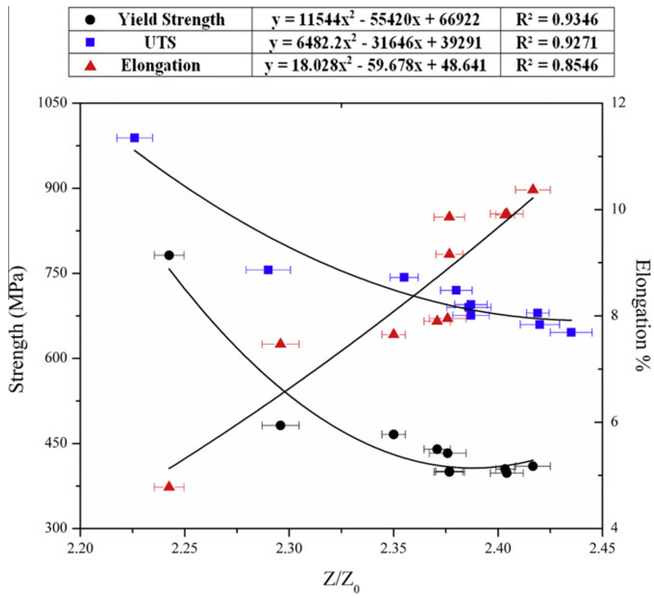

Fig. 7. Relation between the tensile properties of different DPS with normalized impedance.

$$\Pi = \sqrt{\mathrm{Re}^2 + \mathrm{Im}^2} \tag{6}$$

The relationships between martensite phase percentage and different values of harmonics modulus were investigated individually for each harmonic. The values of vector modulus of each harmonic are listed in Table 2. It should be noted that frequency of 375 Hz was chosen as the optimum frequency for harmonic output according to the regression analysis.

The modulus of harmonics is plotted versus the martensite phase percentage (Fig. 5). The values of the vector modulus decrease with an increase in the martensite phase percentages. Magnetic permeability of DPS decreased by an increasing the martensite percentage. As a result, reduction of coil output voltage leads to the decreasing the harmonic values due to the smaller amplitude of the voltage wave at higher martensite phase percentages (Eq. (5)).

Correlation coefficients are also shown in Fig. 5. For all obtained relations, the amounts of correlation coefficients are very high ($0.9558 < R^2 < 0.9742$), which again, confirm the capability of the method as a tool in quality control inspection.

Microstructural changes affect directly the magnetic properties of the materials and their mechanical properties are directly influenced by their microstructures [25]. It is therefore possible to find a beneficial indirect relationship between the magnetic and mechanical properties of DPS samples.

Fig. 6 indicates correlation between the Impedance outputs and the Vickers's hardness values. This method was also used to find a relationship between tensile properties and magnetic properties of DPS (Fig. 7).

An increase in the martensite phase percentage leads to an increase in the Vickers's hardness values, yield and ultimate tensile strengths and to a decrease in the elongation of DPS. In other hand, magnetic permeability of DPS decreases as martensite percentage increase. Thus decrease in the VHN, yield and ultimate tensile strengths while increasing the elongation leads to an increase in the values of impedance.

Two important advantages of using this presented automatic calibration method are the high calibration velocity and the short measuring time for determination of material properties. As mentioned, induced eddy currents are a function of electromagnetic and physical parameters. Fixing of frequency and physical parameters is simple for quality control in a mass production line. However, electrical conductivity and magnetic permeability are the unique parameters that can affect the material characterization. Therefore the presented measuring system is suitable for an online inspection system in a mass production line of DPS.

4. Conclusions

In the present paper, it was found that ECT has a great potential to be used in the production line of DPS so that it can detect undesirable microstructures based on their percentage of martensite in the shortest possible time. It was shown that the eddy current method is very sensitive and well related to martensite phase percentage in DPS and high correlation coefficients confirm these findings ($R^2 > 0.94$). Higher martensite percentage decreases the magnetic permeability of the material and results in the decrease in ECT outputs. Furthermore, this method was used for prediction of mechanical properties of DPS. Microstructural changes affect the magnetic and mechanical properties of DPS and it can obtain beneficial relations between magnetic and mechanical properties of DPS.

In order to be used as a tool for industrial inspection, it needs only to be calibrated on reference samples of known martensite percentage and mechanical properties and then ECT can separate the good samples and the bad ones, carefully.

References

[1] Kim S-J, Cho Y-G, Oh C-S, Kim DE, Moon MB, Han HN. Development of a dual phase steel using orthogonal design method. Mater Des 2009;30:1251–7.
[2] Mazinani M, Poole WJ. Effect of martensite plasticity on the deformation behavior of a low-carbon dual-phase steel. Metall Mater Trans A 2007;38:328–39.
[3] Committee AIH. ASM Handbook, properties & selection: irons, steels, and high-performance alloys: ASM, International; 1990: vol. 01.
[4] Bayram A, Uguz A, Ula M. Effects of microstructure and notches on the mechanical properties of dual-phase steels. Mater Charact 1999;43:259–69.
[5] Ahmad E, Manzoor T, Ali K, Akhter J. Effect of microvoid formation on the tensile properties of dual-phase steel. J Mater Eng Perform 2000;9:306–10.
[6] Marder A. Deformation characteristics of dual-phase steels. Metall Mater Trans A 1982;13:85–92.
[7] Kim N, Thomas G. Effects of morphology on the mechanical behavior of a dual phase Fe/2Si/0 1C steel. Metall Mater Trans A 1981;12:483–9.
[8] Bhagavathi LR, Chaudhari GP, Nath SK. Mechanical and corrosion behavior of plain low carbon dual-phase steels. Mater Des 2011;32:433–40.
[9] Meng Q, Li J, Wang J, Zhang Z, Zhang L. Effect of water quenching process on microstructure and tensile properties of low alloy cold rolled dual-phase steel. Mater Des 2009;30:2379–85.
[10] Shull PJ. Nondestructive evaluation: theory, techniques, and applications: M. Dekker; 2002.
[11] Hellier C. Handbook of nondestructive evaluation. McGraw-Hill; 2001.
[12] Kashefi M, Kahrobaee S. On the application of nondestructive eddy current method for quality control of heat treated parts. In: 18th Congress IFHTSE. Rio de Janeiro; 2010.
[13] Sheikh Amiri M, Kashefi M. Application of eddy current nondestructive method for determination of surface carbon content in carburized steels. NDT & E Int 2009;42:618–21.
[14] Khan SH, Ali F, Khan AN, Iqbal MA. Pearlite determination in plain carbon steel by eddy current method. J Mater Process Technol 2008;200:316–8.
[15] Konoplyuk S. Estimation of pearlite fraction in ductile cast irons by eddy current method. NDT & E Int 2010;43:360–4.
[16] Konoplyuk S, Abe T, Uchimoto T, Takagi T, Kurosawa M. Characterization of ductile cast iron by eddy current method. NDT & E Int 2005;38:623–6.
[17] Yin W, Hao X, Peyton A, Strangwood M, Davis C. Measurement of permeability and ferrite/austenite phase fraction using a multi-frequency electromagnetic sensor. NDT & E Int 2009;42:64–8.
[18] Haldane RJ, Yin W, Strangwood M, Peyton AJ, Davis CL. Multi-frequency electromagnetic sensor measurement of ferrite/austenite phase fraction—Experiment and theory. Scripta Mater 2006;54:1761–5.
[19] Yin W, Peyton AJ, Strangwood M, Davis CL. Exploring the relationship between ferrite fraction and morphology and the electromagnetic properties of steel. J Mater Sci 2007;42:6854–61.
[20] Kahrobaee S, Kashefi M, Saheb Alam A. Magnetic NDT technology for characterization of decarburizing depth. Surf Coat Technol 2011;205:4083–8.
[21] Abbaschian R, Abbaschian L, Reed-Hill RE. Physical Metallurgy Principles: Cengage Learning; 2008.

[22] Gros XE. An eddy current approach to the detection of damage caused by low-energy impacts on carbon fibre reinforced materials. Mater Des 1995;16:167–73.
[23] Bray DE, Stanley RK. Nondestructive evaluation: a tool in design manufacturing and service. CRC Press; 1997.
[24] ASM, International A. ASM Handbook, vol. 17: Nondestructive Evaluation and Quality Control: ASM International; 1989.
[25] Kahrobaee S, Kashefi M. Hardness profile plotting using multi-frequency multi-output electromagnetic sensor. NDT & E Int 2011;44:335–8.
[26] Johnson Marcus, Lo Chester, Hentscher Scott, Emily K. Analysis of conductivity and permeability profiles in hardened steel. Electromagnetic Nondestructive Evaluation (IX): IOS press; 2005.